

# LASER DIAGNOSTICS OF SHOCK WAVES IN EXPERIMENTAL GAS DYNAMICS

Yu.N. Dubnishchev\*, V.A. Arbuzov, P.P. Belousov, P.Ya. Belousov  
Institute of Thermophysics of the Siberian Branch of the Russian Academy of Sciences,  
630090, Novosibirsk, Russia  
E-mail: [dubnistchev@itp.nsc.ru](mailto:dubnistchev@itp.nsc.ru)

## ABSTRACT

Diagnostics of local and field characteristics of moving medium in tasks of gas dynamics measurement of local velocities and fields of velocities in flows, research of dynamic structure of shock waves and the dynamic disturbances induced by a shock wave in the air is discussed.

**Keywords:** Laser Doppler Anemometry, visualization of fields of velocities, shock waves

## 1. INTRODUCTION

The problem of measurement of kinematic parameters of moving medium is general for various fields of science and engineering, among which: experimental hydrodynamics, gas dynamics and research of own oscillations of the Earth and geodynamic disturbances at earthquakes, some industrial technologies (for example, manufacture of metallurgical rolled stock, aerospace and shipbuilding etc.). First of all it concerns the measurement of local velocities, turbulent pulsations and fields of velocities. The optical methods including laser Doppler anemometry [1, 2] are in common used. Qualitatively new diagnostic possibilities are provided by laser Doppler visualization and measurement of a field of the velocities, based on optical discrimination Doppler shift of frequency in a scattered light forming an image of researched section of the moving fluid. This method was offered by authors in [3] and recently has received development under various names from which the most distributed are Doppler Global Velocimetry (DGV) and Planar Doppler Velocimetry (PDV). Laser Doppler visualization of fields of velocities, as against methods PIV (Particle Image Velocimetry), does not demand introduction in the researched fluid of the calibrated particles and identification of their tracks in the images. As to a problem of diagnostics of phase optical density with application shadow and schlieren methods, reserves here are connected to an opportunity of increase of sensitivity and contrast of a pattern for the account Hilbert filtrations of an optical signal. Necessity of nonconventional approaches for optical diagnostics arises in problems non-stationary gas dynamics, connected with research of structure of shock waves, dynamic disturbances, induced by shock waves, with studying zones of turbulent mixing and explosive processes [4–6]. Qualitatively new a level of diagnostic methods is determined by development of multidimensional measuring technologies.

## 2. METHODS AND RESULTS OF RESEARCHES

Possibilities of the diagnostic methods submitted in the report are reflected as a result of their applications in various fields of science and engineering. Among tasks of experimental hydrodynamics researches of the twirled streams, gyroscopic wave structures and jet streams are allocated.

### 2.1. Laser Doppler Visualization of velocity fields in vortex flow.

In Fig. 1 the simplified scheme of an experimental complex is shown. The Ranque–Hilsch tube represents a vortical channel of square section (34 mm x 34 mm) with transparent walls. Airflow enters the tube through a slot–hole swirler. Cold air leaves through the hole in a center of a tube in a plane of the swirler (the “cold” end of the tube). The “hot” end of the tube is made as a radial diffuser. Hot air leaves through this diffuser in radial directions. The mode of operation of the tube was the same as in measurements in the reference [7].

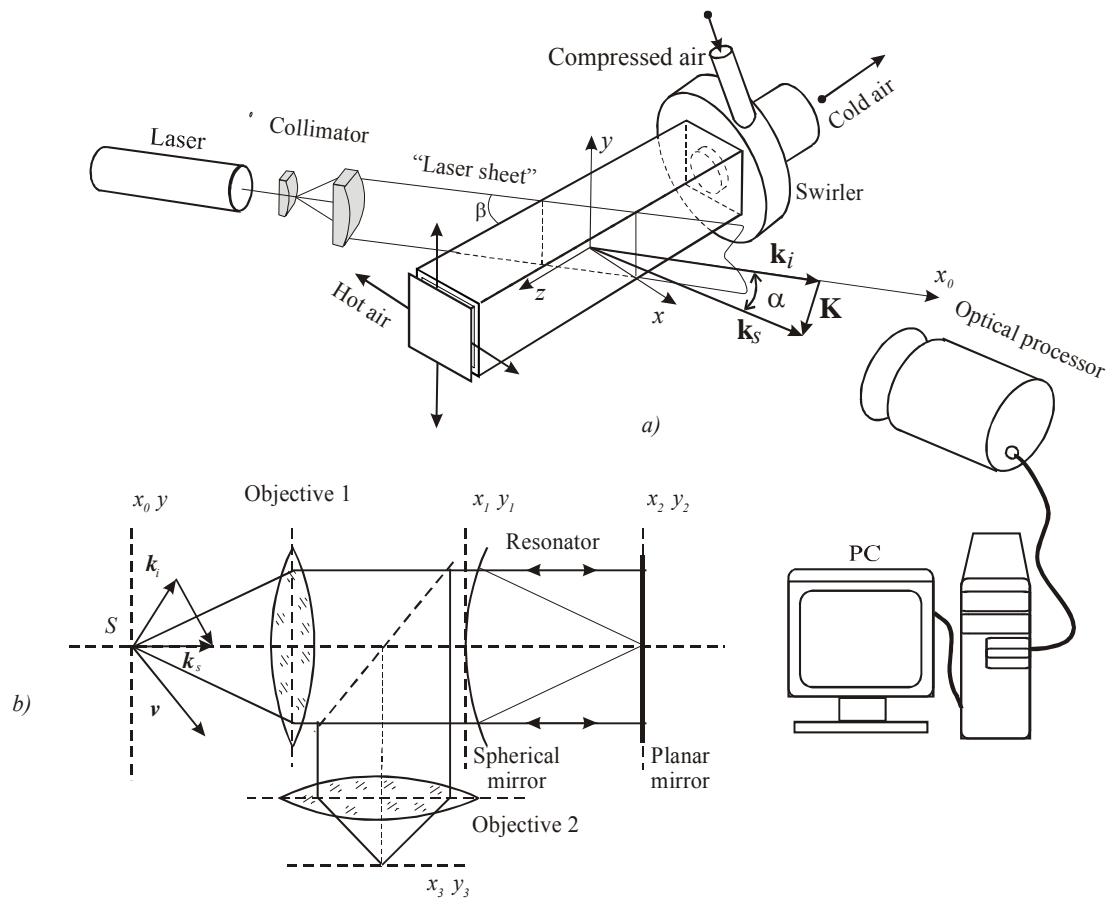


Fig. 1 The function scheme of the experiment: *a*–sketch of the experimental set; *b*–sketch of the optical Doppler processor

The researched section is illuminated by the laser sheet. The source was a helium-neon laser radiated at the basic mode power of 15 mW. The laser sheet was positioned in the plane, orthogonal to horizontal walls at an angle of  $\beta \approx 60^\circ$  to the axis of the tube. The optical axis of the processor forming the image of section illuminated with the laser sheet, was oriented at an angle  $\alpha = 30^\circ$  to the sheet plane. As it follows from the configuration of light beams correlated with the geometry of tube, the spatial distribution of the velocity vector components was visualized in the plane of the laser sheet. The direction of the velocity components was determined by “sensitivity vector”  $\mathbf{K}$ , equal to the difference of wave vectors  $\mathbf{k}_s - \mathbf{k}_i$ , where  $\mathbf{k}_i$  is the wave vector of the beam forming the laser sheet;  $\mathbf{k}_s$  is the wave vector of the scattered beam in the angular spectrum determined by a pass band of the optical processor. The action of the optical processor is described in [2]. The mode structure of the processor is matched with the mode structure of the laser. A transfer function of the processor is of resonant kind. The linear side of a slope of the resonance amplitude-frequency characteristic of the processor is used as the discrimination curve. The processor is based on a semiconfocal optical resonator, the dispersion interval of which is matched to the intermode spacing of the laser. A laser beam is transformed by an anamorphic collimator into planar structure of the “laser sheet” type and directed into the Ranque–Hilsh tube in which a vortical flow is generated with a swirler. The light scattered in the “laser sheet” represents a superposition of waves with Doppler frequency shift proportional to the projection of the velocity of the scattered particles into direction of the difference wave vector  $\mathbf{K} = \mathbf{k}_s - \mathbf{k}_i$ .

An image of the researched section of the flow is formed in the frequency-demodulated scattered light in the output plane  $x_3y_3$  of the optical processor with consecutively positioned objective 1, resonator, objective 2 and is recorded with CCD camera. An intensity of light field in each point of the image is single-valued linear function of the velocity vector projection on the direction of sensitivity vector  $\mathbf{K}$ . The laser radiation frequency is locked to a working on the transfer function of the processor with automatic control system. A signal from output of CCD camera passed to a computer for processing.

Really, the section of the researched fluid illuminated by a beam with a wave vector  $\mathbf{k}_i$  is displayed on the exit of the optical processor as a pattern of images scattering optical nonuniformities  $\varphi(\xi, \eta)\delta(x_0 - \xi, y - \eta)$ , where  $\xi$  and  $\eta$  – are coordinates of the optical nonuniformities (particles) in a plane of the sheet  $(x_0, y)$ . Hence, the frequency-demodulated image of the section produced by the laser sheet with a wave vector  $\mathbf{k}_i$  is able to be described the expression:

$$\omega_D(x, y) = \gamma \iint \mathbf{KV}(\xi, \eta)\varphi(\xi, \eta)\delta(x_0 - \xi, y - \eta)d\eta d\xi = \gamma \mathbf{KV}(x_0, y)\varphi(x_0, y), \quad (1)$$

where the integration is carried out all over the section;  $\omega_D(x, y)$  is a Doppler shift of frequency in light forming a point  $(x_0, y)$  of the image on the output of the optical processor;  $\mathbf{V}(x_0, y)$  is a velocity vector in the point  $(x_0, y)$ ;  $\gamma$  is a steepness of the frequency discrimination characteristic.

The multiplier  $\varphi(x, y)$  corresponds to scattering function in the direction  $\mathbf{k}_s$ . It describes the initial image of the researched section, which has not been subjected to frequency demodulation. Then

$$\tilde{\omega}_D(x, y) = \frac{\omega_D(x_0, y)}{\gamma\varphi(x_0, y)} = \mathbf{KV}(x_0, y)$$

describes distribution of relative intensity of the frequency demodulating image. From this it can be seen, that  $\tilde{\omega}_D(x_0, y)$  unequivocally displays the field components of the velocity in direction  $\mathbf{K}$ :

$$V(x_0, y) = \frac{1}{\mathbf{K}} \omega_D(x_0, y). \quad (2)$$

In Fig. 2, *a-f* there are examples of the visualizing velocity field in a plane of the laser sheet. It can be seen, that the field of velocities contains a change in dynamics of vortical structures, including the structures in the form of coupled vortex spiral. The initial image of the researched section, which has not been subjected to frequency demodulation (*g*) and the schlieren photography (*h*) have been shown. In Fig. 3 the stereoscopic reconstructed distribution  $\mathbf{V}(x_0, y)$  of projections of the vector of velocity on the direction of vector of sensitivity  $\mathbf{K}$  in the plany of the “laser sheet” is given.

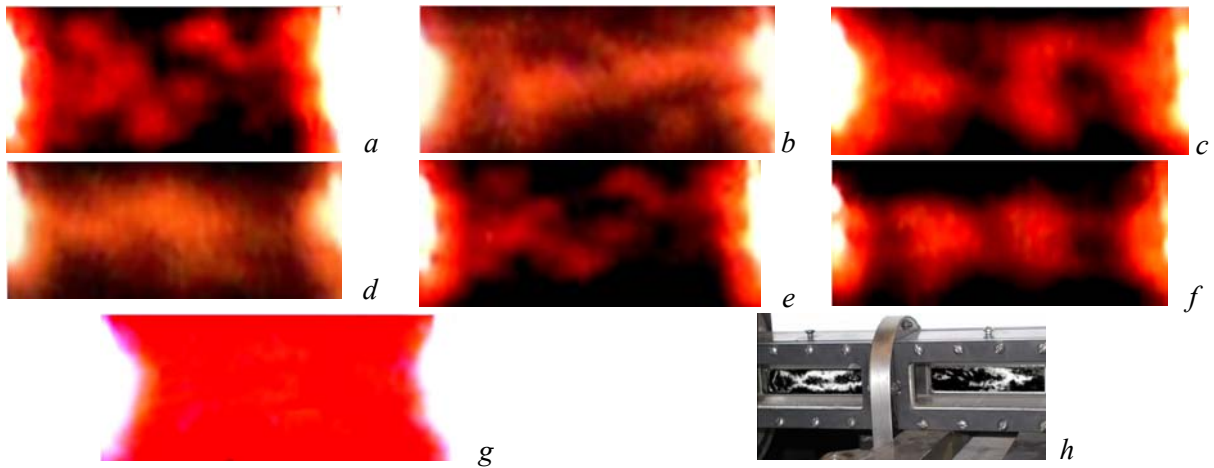


Fig. 2 Examples of the velocities fields in the Ranque vortex flow (*a-f*); the initial image which has not been subjected to frequency demodulation (*g*), the schlieren photography (*h*).

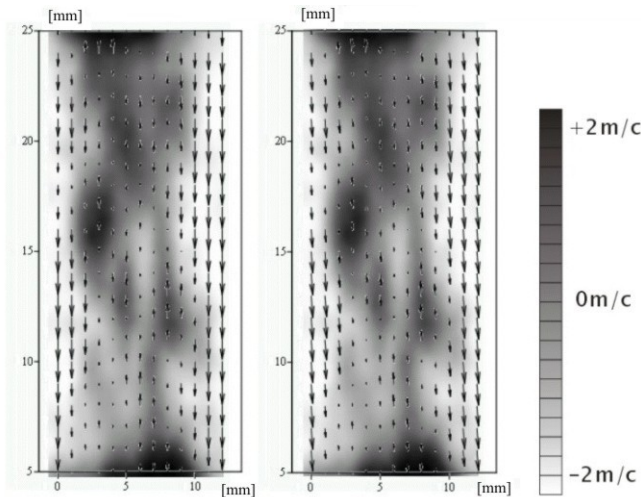
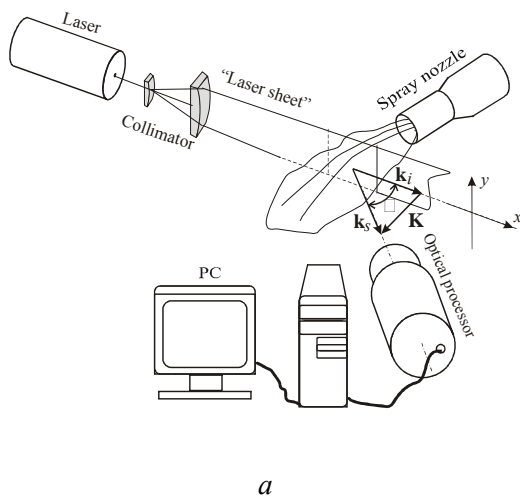
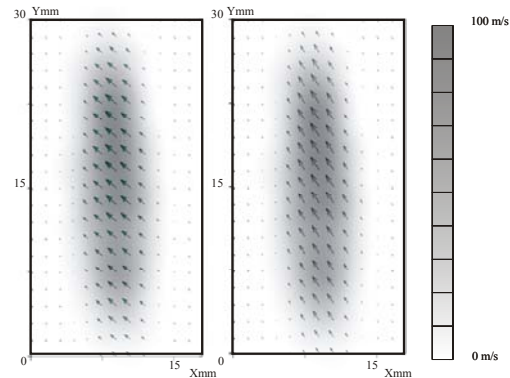


Fig. 3 The section near the hot end of the tube Ranque–Hilsch. Stereoscopic reconstruction of velocity field

velocities is received by laser Doppler visualization method with application of the optical processor with a coherent feedback [2]. The opportunity of visualization and measurement of fields of velocity vectors in three-dimensional orthogonal basis also is theoretically and experimentally proved [2].



*a*



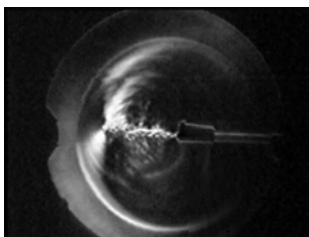
*b*

Fig. 4

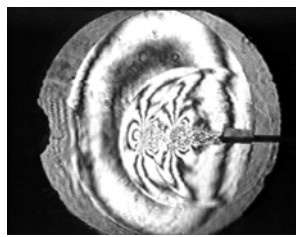
## 2.2. Optical diagnostics of shock waves

The investigations into shock waves and related perturbations in gaseous media are among the most difficult tasks of experimental gas dynamics [4]. This is about the observation of dynamic structures formed at the shock wave front in air.

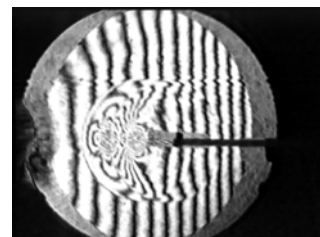
The experiments were performed in a small-size shock tube based on an air gun of the Izh–53 type with a barrel of  $d = 4.5$  mm caliber and 200 mm length. The shock wave was generated upon breakage of a diaphragm made of one or two layers of a 0,05–mm–thick aluminum foil. The use of an air gun as a portable shock tube provides for the simplicity and high efficiency of experiments.



*a*



*b*



*c*

Fig. 5

In Fig. 5 it is shown schlieren pattern reflecting process of distribution of a shock wave (*a*) and shift interference pattern (*b* and *c*), received with application modified shadow device IAB 463 [2] with diameter of observing field 400 mm. In figures the front shock wave, dynamic disturbances and helicoid vortical structure in a direction of an axis of the channel is well seen.

The shock wave diagnostic setup was based on a Pulsar-3M laser Doppler anemometer (LDA) [6] intended for the measurement of 2D flow velocities in gaseous and condensed media in a range of up to  $10^3$  m/s. A special feature of this instrument is a high upper boundary of the dynamic range of velocities, which makes possible the investigation of high-rate nonstationary processes in the frequency range up to 250 MHz. The experimental setup consisted of a mechano-optical unit and a computer-controlled high-speed data acquisition and processing system. The radiation source was a 15-mW He-Ne laser, but the setup can operate (without significant modification) using other laser radiation sources, including semiconductor laser diodes emitting in the visible and near-IR spectral ranges.

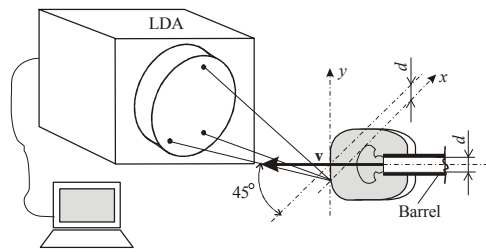


Fig. 6. Schematic diagram of the experimental arrangement (see the text for explanations)

Fig. 6 shows a sketch of the experimental arrangement, with a barrel axis oriented at an angle of  $45^\circ$  relative to the  $xy$  plane of a 2D base coordinate system set by the probing laser field in the LDA frame. Each realization of the process was used to measure one of the two orthogonal components of the velocity vector. Optical channels forming the 2D base coordinate system were switched by acousto-optical modulators of the running wave, which operated according to a preset program or under the action of an external control signal. The ultrasonic wave frequency in the modulators was 80 MHz. The dynamic structure of a probing laser field

formed in the LDA (Pulsar-3M) was such that the array vector coinciding with the direction of motion of the interference fringes was oriented in the opposite direction relative to the measured components  $v_x$  and  $v_y$  of the shock wave velocity vector. For this reason, the Doppler shift equal to the carrier frequency  $f_0 = 80$  MHz in the light scattered from the dynamic structure corresponded to a zero velocity. The probing field was localized within a volume bounded by an ellipsoid with a semiminor axis of  $25 \mu\text{m}$  and a semimajor axis of  $0.35$  mm.

The Doppler signal is formed when the shock wave front travels through the probing field. This signal has the form of a short video pulse with the envelope modulated at a frequency determined by a periodic structure of the probing field and the corresponding component of the shock wave front velocity.

In fig. 7 examples of fragments of realization laser Doppler signal, appropriate to transit of a shock wave through the probing field located on distance of 10 calibers from a cut of the gun trunk are shown. The shock wave was formed at break a diaphragm executed of the two-layer aluminum foil. Fig. 7,*a* and 7,*b* show a Doppler signal from front shock wave in various time scales. On fig. 7,*b* the structure of a signal generated at crossing of probing field by front of a shock wave is well visible. The signal represents the short video impulse. Its envelope is modulated by the frequency determined by structure of probing field and  $x$ -component of velocity of the shock wave. A width of the pulse on the average is about  $0,2 \mu\text{s}$ . The mean velocity of the shock wave for this time interval is equal to  $420$  m/s. In fig. 7,*c* the arrow shows a spectrum of the Doppler signal appropriate  $x$ -component of velocity of the shock wave on the spatial interval determined in the size of probing field on an axis  $x$ . Value of velocity normal to a plane of wave front easily turns out multiplication of value  $x$ -components of velocity on  $\sqrt{2}$ . If all surface of wave front represents casual distribution scattering nonuniformities the estimation of duration of a signal  $2d/v_x$  gives size about  $2 \mu\text{s}$  (here  $d$  is length of big semiaxis of the ellipsoid limiting the probing field). Thus, actual duration of signals at crossing probing field by a shock wave appears on the order less expected in the assumption, that all surface of wave front is covered of scattering noninformies. The conclusion from here follows that the light signal is formed as a result of scattering from the limited local structure at the front of the shock wave. The additional information confirming or refuting this assumption might give measurement  $y$ -components of velocity at the front of the shock wave.

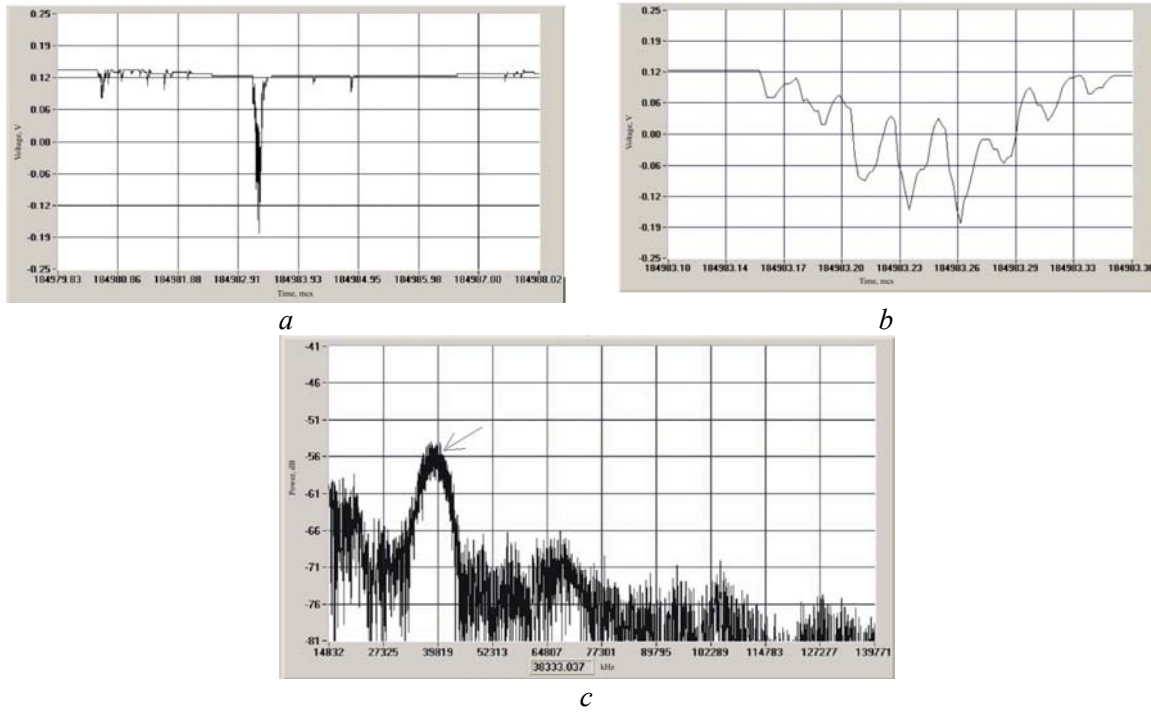


Fig. 7

Kinematic perturbations in the shock wave structure must be manifested in the dynamic velocity. In order to measure this velocity, the base coordinate system set by the probing laser field was oriented so that the  $y$ -axis would be parallel to the wave front velocity.

Fig. 8 shows an example of the typical time series of the Doppler signal observed during the measurement of the  $y$ -component of the velocity vector in the plane of the shock wave front. The probing field was localized at a distance of the barrel edge. The existence of the  $y$ -component of the velocity vector in the configuration of Fig. 8 is indicative of the fact that laser radiation is scattered from the optical inhomogeneities moving in the plane of the wave front.

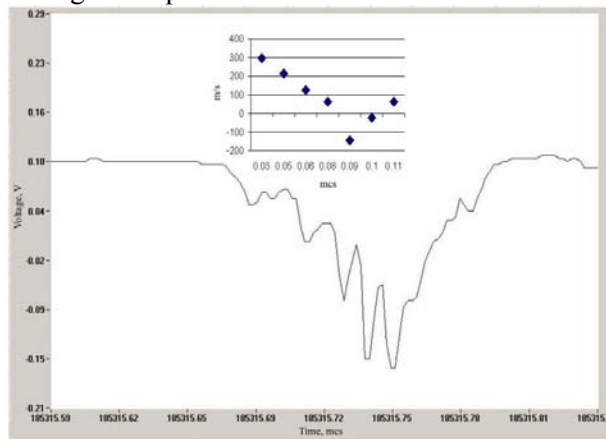


Fig. 8. A fragment of the time series of a Doppler signal obtained for they component of velocity in the shock wave front plane. The inset shows the time variation of the local velocity of motion of the dynamic scattering structure formed at the shock wave front.

The shape of the Doppler signals corresponding to the  $y$  component of the velocity vector is indicative of the ordered structure of dynamic perturbations at the shock wave front. The inset in Fig. 8 shows the time variation of the local velocity of motion of the dynamic scattering structure formed at the shock wave front. The time intervals corresponding to the measured signal and the dynamic velocity are mutually consistent. As can be seen from Fig. 8, the envelope of the Doppler signal is modulated at a variable frequency. The measured velocity is a single-valued function of this frequency. The velocity varies from 300 m/s to zero over a 0.08  $\mu$ s time interval and then changes the sign. One possible explanation is that a signal of this type can be due to the scattering of a probing field on a tangential rotating structure.

In order to reveal the structure of the shock wave front, we performed special experiments using a 2D “laser sheet”, which was formed by radiation of a 200 mW argon laser ( $\lambda = 0.515 \mu\text{m}$ ) at distance of  $20d$  from the barrel edge. The shock wave was initiated by the breakage of the diaphragm made of single-layer aluminum foil. The shockwave crossing the laser plane was monitored using a CCD camera. Fig. 9,*a–b* shows an examples of the image of a shock wave front crossing the laser sheet, which clearly reveals the radial–tangential mode structure of optical density and is indicative of the possible oscillatory nature of such structures.

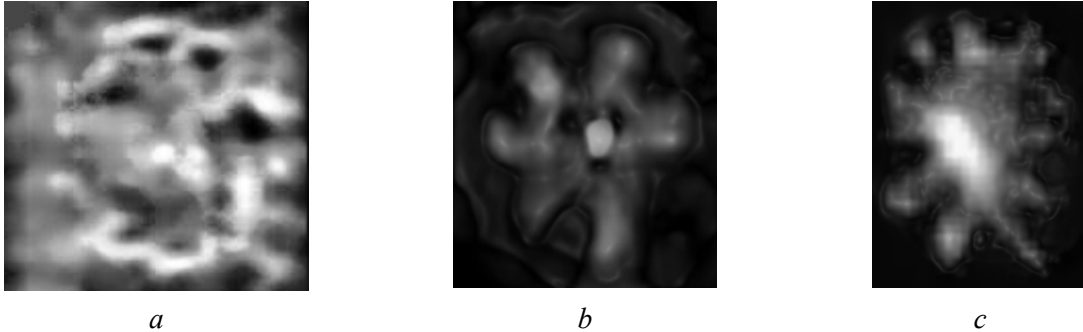


Fig. 9

Existence of radial and tangential dynamic structures on wave front of the shock wave, revealed by methods laser Doppler anemometry and laser visualization of optical density proves to be true the following simple experiment. The shock wave formed by a shot of the pneumatic gun went on a flat surface of a layer of the modeling clay placed on a rigid plate. In Fig. 10,*a–c* prints of shock waves are given (the surface of the modeling clay settled down on distance of  $10d$  from a cut of a trunk). Radial and tangential structures are well visible. These structures are similar oscillatory modes.

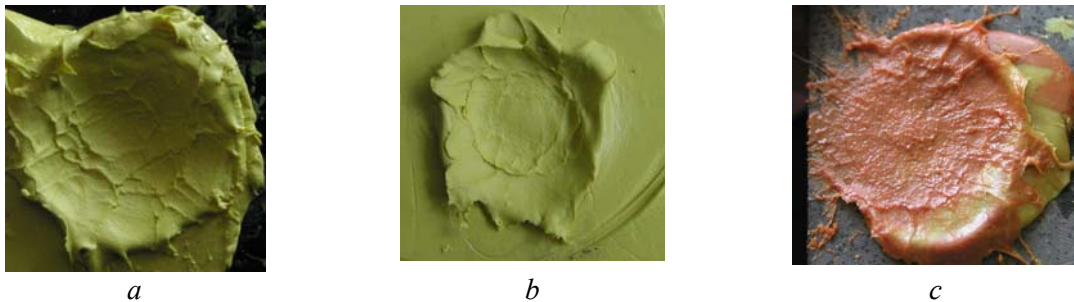


Fig. 10

As indirect confirmation of a hypothesis on an oscillatory nature of the structures on wave front of a shock wave can be found on the photos of craters on a surface of the Moon (Fig. 11).

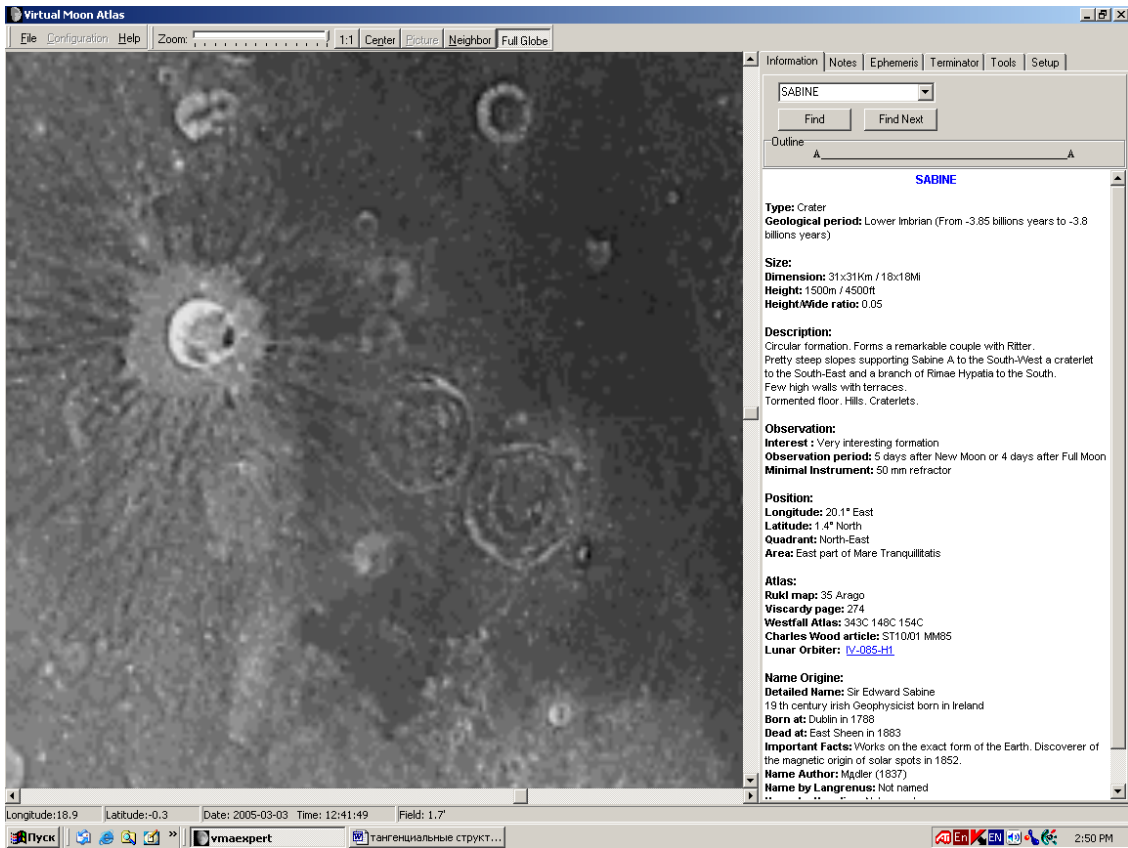


Fig. 11

In Fig. 12,*a-d* examples of typical images of some lunar craters close up are shown. In a configurates with a surface of Moon should be displayed. Difference of these structures is determined by the various energy allocated at collision.

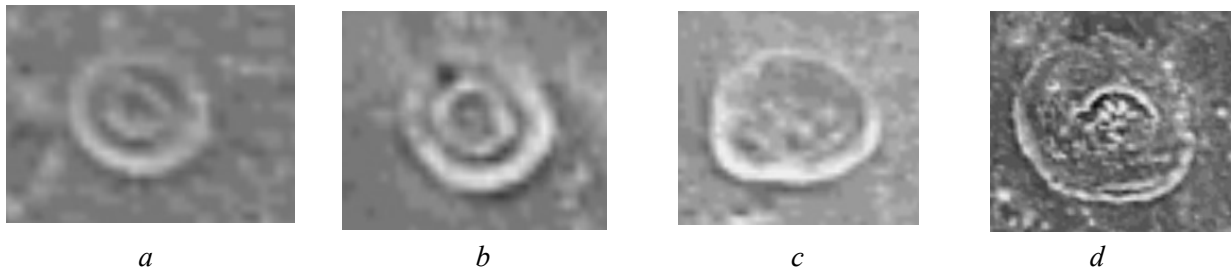


Fig. 12

Fig. 13,*a-b* show the structure of front of the shock wave (*a*) received by a method of laser visualization of dynamic density (Fig. 13,*a* is identical Fig. 8,*a*) and the structure of the Chebyshev crater (*b*) on the Moon. Similarity of these structures associates with structure of an oscillatory mode.



Fig. 13

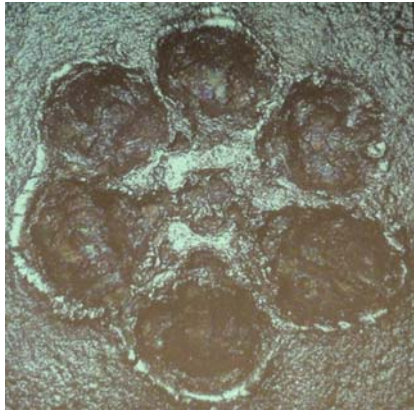


Fig. 14

Above mentioned results will be coordinated to photos of imprints received at collision of metal plates with a flat massive obstacle moving with high speed ( $\sim 11$  km/s) (Fig. 14). This stamp was shown by academician G.G. Cherny at Intern. Conf. “High-speed flow fundamental problems” (Zhukovsky, TSAGI, 2004).

The LDA (Pulsar-3M) was used for the investigation of dynamic perturbations produced in air by the propagating shock wave. The particles and optical inhomogeneities crossing the probing field produce random discretization of a nonstationary process, which reflects the dynamic state of the medium in the spatial region within the localized probing field. Computer processing of the signal corresponding to a random sampling provides information on the local velocity field

evolution during the shock wave propagation in air fluid.

Figure 15 shows the typical time variation of the local velocity in air perturbed by the shock wave. The measurements were performed in the geometry depicted in Fig. 6.

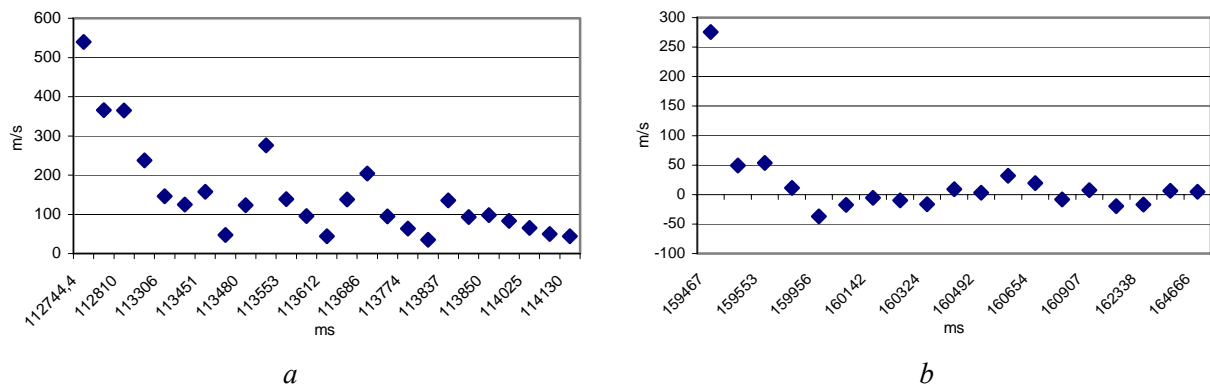


Fig. 15

The probing field was localized at a distance of  $10d$  from the barrel edge. The velocity component was measured along the  $x$ -axis in the shock wave propagation direction (Fig. 15,*a*) and along the  $y$ -axis parallel to the shock wave front plane (Fig. 15,*b*). These data illustrate the evolution of orthogonal components of the local velocity in air perturbed by the shock wave.

### 3. CONCLUSION

Functional possibilities of the developed methods of diagnostics of kinematic and structural parameters of dynamically disturbed medium are illustrated by reception of qualitatively new results in hydrodynamics and gas dynamics.

### ACKNOWLEDGMENTS

The authors are grateful to E.E. Meshkov, A.L. Mikhailov, and V.M. Titov for support and fruitful discussions. This study was supported by the Russian Foundation for Basic Research (project no. 05-02-16896) and the Siberian Division of the Russian Academy of Sciences (integration project no. 28).

### REFERENCES

- [1] Dubnishchev J.N., Rinkevichjus B.S. *Methods Laser Doppler Anemometry* (in Russian). 1982, M.: Nauka, 306 p.
- [2] Dubnishchev J.N., Arbutov V.A., Belousov P.P. and Belousov P.Ya. *Optical methods of research of streams* (in Russian). Novosibirsk: the Siberian university publishing house, 418 p. 2003.
- [3] Belousov P.J., Dubnishchev J.N., Pal'chikova I.G. *Visualization of a field of velocity in field* (in Russian) // *Optics and spectroscopy*. V. 52, No 5, pp. 876-879, 1982.

- [4] L. Hous, T.T. Vtirjd, and G. Jourdan. *Shock Vaves*. No 9, 249, 1999.
- [5] Dubnishchev Yu. N., Arbuzov V.A., Belousov P.P., Belousov P.Ya., Meshkov E.E. *Laser Doppler diagnostics of nonstationary high velocity streams*. Proc. Intern. Conference VII Kharitons topical scientific readings. Extreme states of substance. Detonation. Shock waves. Sarov, p. 311, 2005.
- [6] P.P. Belousov, P.Ya. Belousov, Yu. N. Dubnishchev. *Optical Diagnostics of Dynamic Structures in Shock Waves*. Technical Physics Letters, Vol. 31, No 11, pp. 973–975, 2005.
- [7] V.A. Arbuzov, Yu. N. Dubnishchev, V.A. Lebedev, M.Kh. Pravdina, and N.I. Yavorski. *Observation of large-scale hydrodynamic structures in vortex tube and the Ranque effect*. Technical Physics Letters, 23, 938, 1997.